EFFECT OF THE LAMBDA PARAMETER ON THREE-PHASE INDUCTION MOTOR DESIGN BY ANALYTICAL AND MAGNETIC METHODS

ASIM GÖKHAN YETGIN1, MEHMET MURAT TEZCAN2

Keywords: Induction motor design; Lambda value; Performance analysis; Magnetic analysis.

Induction motors can be designed for powers ranging from small to considerable. Several key parameters must be considered during the design process. In addition to critical motor design parameters, there are also design parameters that are often overlooked and are typically assumed to be a fixed or average value. One of these parameters is the λ (lambda) parameter, which represents the ratio of the package length to the pole pitch. This parameter is typically specified in design books and appears to be a subject that researchers rarely study. In this study, a 7.5 kW, 3-phase squirrel-cage induction motor has been designed using the lambda value to fill the gap in the literature. The primary motivation of this study is to demonstrate how the lambda value influences the dimensions of the motor and its impact on the performance and magnetic performance of the motor. For this purpose, analytical and 2D modeling have been performed using Rmxprt and Ansys Maxwell software for motor analysis. Performance and magnetic analyses were performed. According to the results obtained, it is concluded that the lambda coefficient, which is not very important in the design process, is a very effective parameter in motor design.

1. INTRODUCTION

Three-phase induction motors are the most widely used machines in industrial applications [1], [2] and worldwide [3] due to their cheap and reliable operation [4], simple construction, and easy operation [5]. Various design techniques have been established to maintain its current position as the workhorse of the industry. One of the most common methods in the design of electrical machines is the D^2L method, which was initially developed for constant-speed motors and provides favorable efficiency and size. Since this method is based on machine theories and a long history of empirical data, it is beneficial and accurate in the design of constant-speed machines [6]. The D^2L expression is a measure of the physical volume of the machine. In the first stage, the D^2L expression should be determined approximately when designing the motor. In the latter process, this expression is divided into two components, D and L, and the operations are carried out [7].

When designing an induction motor, motor designs of different types and sizes can also be realised to meet the features and needs of the customer, which require a special design. For this reason, it is necessary to know/calculate the exact size of all parts of the motor to be designed. When designing a motor, the dimensions of the stator, including the stator package length and diameter, the details of the stator windings and stator slots, the design details of the stator and rotor slots, and the performance of the motor are of great importance. To obtain the design details, the designer requires the necessary customer specifications, including rated power output, rated voltage, speed, frequency, stator winding type and connection, rotor winding type, operating conditions, and shaft length, among others [8]. The design of these motors involves many processes, such as the selection of materials to be used, production, testing, control of performance values, etc. Electromagnetic calculation is an essential part of the motor design process that defines/calculates various parameters such as voltage, current, flux, inductance in the magnetic core, teeth, yoke, coils, etc. [9].

To enhance the performance of induction motors, various design methods and optimization techniques are available, and researchers are continually working to achieve optimal performance from the motor.

In his study, Dinh optimized the design of the outer diameter, inner diameter, package length, stator, and rotor slot shapes of a 2200 W, 4-pole induction motor to reduce stator and rotor

copper losses and iron losses [10]. Akhtar and Behera analyzed the effects of variations in stator and rotor slot dimensions on the efficiency, maximum torque and power factor of an induction motor. They optimized the stator and rotor dimensions with the genetic algorithm method to improve the motor performance [11]. Benallal et al. have designed an induction motor that will allow the optimum use of the active parts of the motor by considering the value of the air gap flux density variation [12].

In his book, Boldea categorized the design of an induction motor under five headings in general. These are electrical, magnetic, mechanical, insulation, and thermal designs [13]. In their study, Aishwarya and Brisilla analyzed how the motor performance changes when different materials and different winding types are used in the core of an induction motor using Ansys and Rmxprt programs [14]. Onwuka et al. analyzed how the motor performance of 3 induction motors with the same electrical characteristics changes at different air gap values [15]. Some of the studies on improving motor performance by designing/optimizing/improving/modelling, etc., of various parameters of induction motor are summarized and given in Table 1.

Table 1
Summary of the studies on induction motor design

Summary of the studies on induction motor design					
Subjects	References	Subjects	References		
Stator windings	[16], [17] Parameters of rotor slot		[25], [26], [27]		
Unbalanced voltage	[18], [19]	Optimization	[28], [29], [30], [31],		
Different rotor material	[20]	Number of rotor slot	[32], [33], [34], [35]		
Different rotor	[20], [21],	[20], [21], Number of			
slot structure	[22], [23] stator slot		[36]		
Slot wedge	[24]	Change of airgap	[37], [38], [39]		
Parameters of stator slot	[11], [25]	Change of package length	[10]		
Analytical optimization of lambda parameter			In this study		

In this study, it is investigated how the lambda parameter, which is one of the design parameters of a 3-phase squirrel cage induction motor, affects the motor performance. In the first stage, D and L values of an existing motor are changed, and new D^2L output coefficients are obtained. By means of these expressions, the necessary parameters were analytically calculated. In the next stage, these data were

DOI: 10.59277/RRST-EE.2025.70.4.1

¹ Burdur Mehmet Akif Ersoy Unv., Dept. of Electrical Electronics Eng., 15030, Burdur, Türkiye. E-mails: agyetgin@mehmetakif.edu.tr (correspondence), murat.tezcan@dpu.edu.tr

integrated into the Rmxprt [40] programme. Motor designs were obtained for each lambda value from the programme. 2-D models of the motors were created, and magnetic and transient analyses were performed with Ansys Maxwell. The data from the nine new motor models (from lambda 1.0 to 1.8) were compared with the original motor and interpreted.

2. MATERIALS AND METHODS

Although many parameters play an active role in the design of induction motors, it should not be forgotten that motor design is an interdependent process. In other words, only proper stator design or only optimum windings do not mean that the performance of the motor will be maximum. Induction motor design is a complex process based on hundreds of formulae, and the effect of each design parameter on motor design and performance is of different intensity. In particular, motor design companies and software can design induction motors based on basic parameters such as entering the desired label values of the motor, outer/inner diameter values, winding properties, stator and rotor geometric dimensions. However, there are parameters that are not taken into account much during the design phase, and one of these critical parameters is the lambda (ratio of package length to pole pitch) value. This value is tabulated in design books based on past experiences and the design process is continued by taking an average value.

In general, the design process of induction motors starts with the determination of flux densities and current densities and continues with the calculation of the stator inner diameter, package length, stator slots, and stator outer diameter after the stator and rotor currents are found. Rotor slot, rotor yoke height, and cage dimensions are calculated, and motor design is continued [41]. In the following stages, winding sizing, performance analyses, magnetic analyses, and thermal analyses are performed, and the design process is completed. If the desired/targeted values are not achieved, the motor design process continues by recalculating all parameters by assigning new values from the beginning.

In this study, the flow diagram of the motor design process is given in Fig.1.

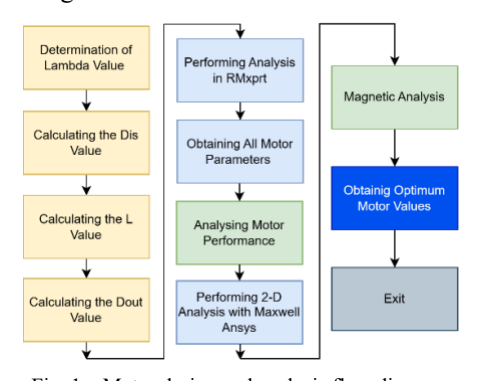


Fig. 1 – Motor design and analysis flow diagram.

2.1 GEOMETRIC FORMULATION

The equation D_{is}^2L is a well-known standard formula based on Faraday's law and the assumption that the machine generates a sinusoidal electromotive force. It relates the output power P_n and synchronous speed n_s to the stator inner diameter D_{is} and the package length L as follows [42].

$$\frac{P_n}{n_c} = C_0 \cdot \eta \cdot \cos\theta \cdot D_{is}^2 L. \tag{1}$$

 $\frac{P_n}{n_s} = C_0 \cdot \eta \cdot \cos\theta \cdot D_{is}^2 L. \tag{1}$ In the equation, C_o is the Esson constant, η is the efficiency, and $\cos\theta$ is the power factor. If the expression in

eq. (1) is elaborated, the following equation is obtained [13].

$$D_{is}^{2}L = \frac{1}{C_{0}} \frac{60}{n_{s}} \frac{K_{e}*P_{n}}{\eta \cdot \cos \theta}.$$
 (2)

 $D_{is}^{2}L = \frac{1}{c_{0}} \frac{60}{n_{s}} \frac{K_{e}*P_{n}}{\cos \theta}. \tag{2}$ If the $D_{is}^{2}L$ expression is separated, the stator inner diameter value can be calculated as given in eq. (3) [41].

$$D_{is} = \sqrt[3]{\frac{2p}{\pi\lambda} \frac{1}{C_0} \frac{p}{f} \frac{K_e * P_n}{\eta \cdot \cos\theta}}.$$
 (3)

In the equation, p is the number of poles, $\lambda(\lambda)$ is the ratio of package length to pole pitch, and f is the frequency. As it is seen, the stator inner diameter value varies depending on many parameters, and one of these parameters is the lambda parameter, which is given in eq. (4) [41]. In the expression, τ determines the pole pitch.

$$\lambda = L\left(\frac{2 \cdot p}{\pi D_{is}}\right) = \frac{L}{\tau}.\tag{4}$$

This expression varies between 0.6 and 3.0 depending on the number of poles [10], and its variation based on experience is given in Table 2 [41].

Variation of λ according to the number of poles.

2p 4 1.2 - 1.8 1.6 - 2.2 0.6 - 1.0

In this table, it should be noted that the maximum value of the lambda parameter is 1.0 for the 2-pole motor, and the minimum value is 1.2 for the 4-pole motor. It is seen that the values between 1 and 1.2 of the lambda value do not correspond to any number of poles. On the other hand, it is seen that some lambda values for 6-pole and 8-pole motors coincide with the values for other pole numbers. One of the most important parts of this table is that no lambda value is defined for motors with poles larger than 8-pole motors.

It was stated by Boldea and Nasar that the value of λ varies from 0.6 to 3. In general, a longer package length allowing a smaller stator diameter leads to shorter stator winding end connections, lower winding losses, and lower inertia. However, the temperature rise along the package length can become significant. The optimum value of λ is highly dependent on the design characteristics of the induction motor and the objective function considered [43].

The value of λ is usually used to separate D_{is}^2L into D_{is} , the stator diameter value, and L, the package length. While the range of 1.2 - 1.8 is given for 4-pole machines in various design books, it is stated that λ is taken as 1.5 for a 5.5 kW motor, λ is taken as 1.1 for a 736 kW motor, λ is taken as 1.3 for 2.5 MW, and λ is taken as 1 for a 7.5 kW motor [44].

Different ranges of λ are given in Table 3 to obtain different design results in various design books.

Table 3 λ ranges for different motor designs

	Ref. [45]	Ref. [46]	Ref. [47]
Good power factor	1.0 - 1.3	1.0 - 1.5	1.0 - 1.25
Overall/balanced design	1.0 - 1.1	1.0	1.0
Good efficiency	1.4 - 1.6	1.5	1.5
Minimum cost	1.5 - 2.0	1.5 - 2.0	1.5 - 2.0

Also, λ values as low as 0.6 can be used for 2-pole machines with a rated power of a few kilowatts and for some smaller power machines [46]. Olubamiwa, on the other hand, stated that the value of λ offers solutions in a wider range of 0.6 - 4 in different design books [44].

Based on the lambda parameter, the stator package length can also be calculated and is given in eq. (5).

$$L = \lambda \left(\frac{\pi * D_{is}}{2p} \right). \tag{5}$$

The other stage of the design process is to determine the stator outer diameter (D_{out}) value. This expression is given in eq. (6) [13].

$$D_{out} = \sqrt{\frac{2p^2}{\pi \lambda C_0 f} \frac{K_e P_n}{\eta \cos \theta} \frac{1}{D_{is} f(D_{is})}}.$$
 (6)

After the general framework of the motor is determined, other parameters such as stator winding design, stator and rotor slots design are calculated, and this process continues until the desired targets are achieved.

As can be seen from the equations, the lambda parameter has a considerable effect on the design parameters of the motor. For this reason, it is of great importance to select the appropriate lambda value. In addition, the lambda value is included in induction motor design books, and there is almost no publication in the literature showing the effect of this parameter. For this reason, the data obtained in this study will contribute to determining the lambda value and to the existing literature on which parameters the lambda affects in induction motor design.

2.2 MOTOR SPECIFICATIONS AND MODELS

The motor type analysed is 132 Frame, which is a widely used motor size in Türkiye and Europe. The nameplate values of the original motor analysed are given in Table 4.

Table 4
Induction motor nameplate values

Parameters	Values	Parameters	Values
Power	7500 W	Connection type	Delta
Voltage	415 V	Number of poles	2
Frequency	50 Hz	Speed	1440 rpm
Power factor	0.84		

The 2-D representation and stator/rotor slot geometry of the analysed motor are given in Fig. 2.

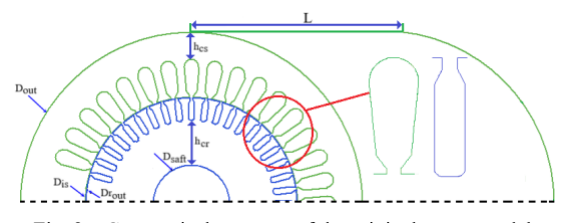


Fig. 2 – Geometrical structure of the original motor model.

The geometrical dimensions of the original motor are given in Table 5.

Table 5
Geometric dimensions of the original motor model

Parameters	Values	Parameters	Values
St. outer diameter	230 mm	Package length	134.8 mm
St. inner diameter	143 mm	No. of stator slot	36
Air gap length	0.4 mm	No. of rotor slot	44
Core material	M270-50A		

The lambda value of the original motor was selected as 1.2. To examine the effect of lambda on the motor design and performance, nine motor models were created by starting from 1.0 and increasing the lambda value up to 1.8. For a clearer understanding of the difference between the geometries, only the lambda 1.0 and the lambda 1.8 motor models are given. In Fig. 3, 3-D visuals of lambda 1.0 and lambda 1.8 motor models are given. It is seen that the lambda

value has a significant effect on the dimensioning of the motor. In addition to the change in diameter and package length, it is understood that many critical parameters, such as the tooth widths between the stator and rotor slots, stator and rotor yoke lengths, are affected.

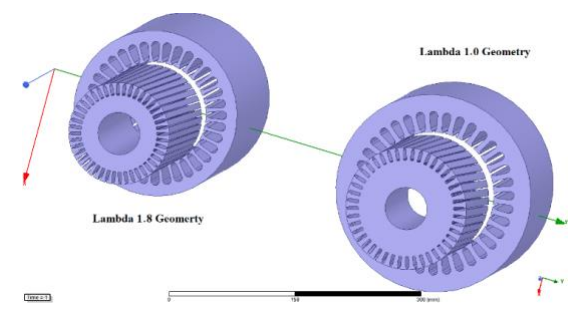


Fig. 3 - 3-D representation of the modelled motor models.

3. OBTAINED RESULTS

The RMxprt results and 2-D results obtained depending on the change of lambda are given in this section. The effects of the lambda value on the geometric dimensions of the motor are given in Fig. 4.

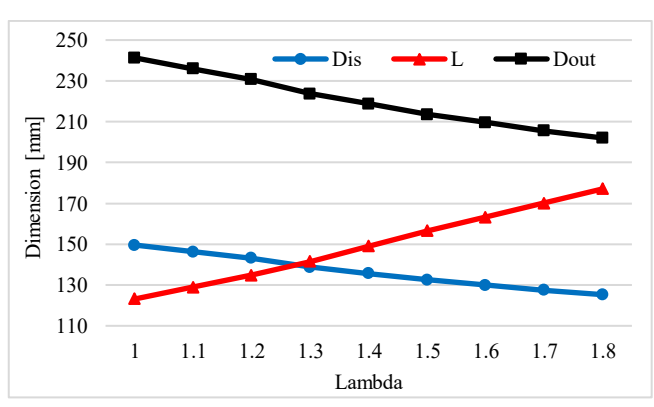


Fig. 4 – Lambda versus D_{is} , D_{out} , and L graph.

Here, it is seen that the D_{is} , L, and D_{out} parameters calculated with the help of the equations given above change with lambda at large rates. It is seen that the stator inner diameter value and the stator outer diameter value decrease, while the package length increases at a large rate. It is observed that the motor transitions from a large-diameter, small-length motor to a small-diameter, large-length motor as the lambda value changes. This situation is clearly seen in the 3-D images given in Fig. 3.

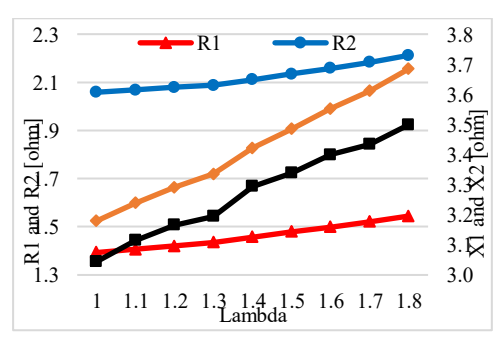


Fig. 5 – Variation of lambda-equivalent circuit parameters.

The effect of lambda on the stator resistance and reactance (R_1, X_1) and rotor resistance and reactance (R_2, X_2) is given in Fig. 5. When the figure is examined, it is seen that with the increase in the lambda value, a significant change occurs in the

equivalent circuit parameters, and the value of each parameter increases. It is seen that the reactance values increase more than the resistance values.

The graph shows the change in stator and rotor copper losses (P_{cus}, P_{cur}) and iron losses (P_{fe}) with the lambda change, as given in Fig. 6. When the figure is examined, it is seen that the stator and rotor copper losses increase depending on the increase in resistance values, while the iron losses decrease.

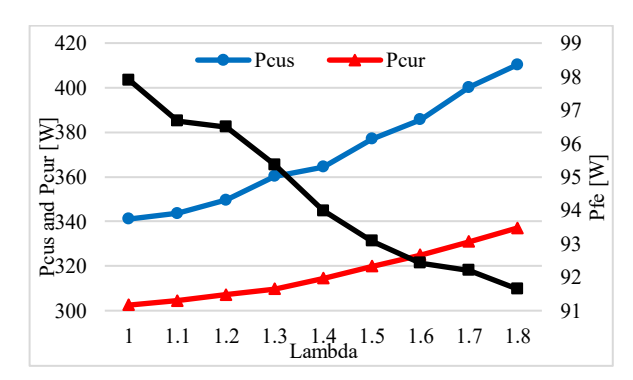


Fig. 6 – Change of lambda-loss powers

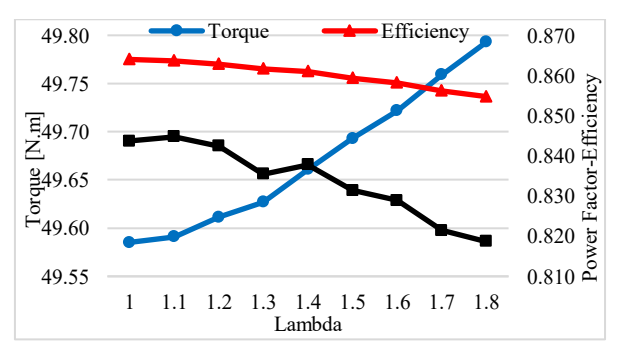


Fig. 7 – Lambda versus torque-power factor and efficiency graph.

Motor performance changes are given in Fig. 7. When the figure is examined, it is seen that the biggest change is in the power factor value. It is seen that there is a 0.94% decrease in efficiency with the increase in lambda. It is understood that the change in lambda has no effect on the nominal torque value.

In Fig. 8, the stator and rotor tooth flux densities (B_{st} , B_{rt}) and yoke flux densities (B_{sy} , B_{ry}) and the flux density in the air gap (B_{ag}) values obtained analytically at different points of the motor are given. When the figure is examined, it is seen that there is a slight increase in the flux density values. The reason for this is that, with the increase in the lambda value, the stator and rotor tooth width and yoke values, depending on the decrease in the motor outer and inner diameter values, are reduced. Saturation has occurred in these parts.

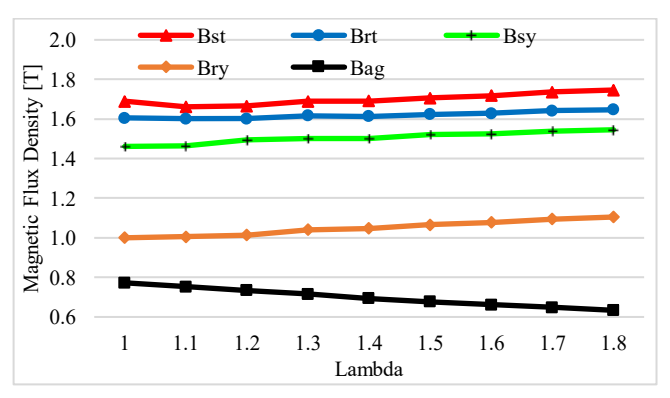


Fig. 8 – Lambda-magnetic flux density variation.

In Fi. 9, the stator and rotor core weights obtained according

to lambda values and the change in the total weight of the motor are given. The decrease in the outer and inner diameter values with the increase in the lambda value resulted in a slight decrease in the stator and rotor core weight. A decrease occurred in the total motor weight value with the increase in lambda. While calculating the total weight values, values such as winding, insulation, etc., were also considered.

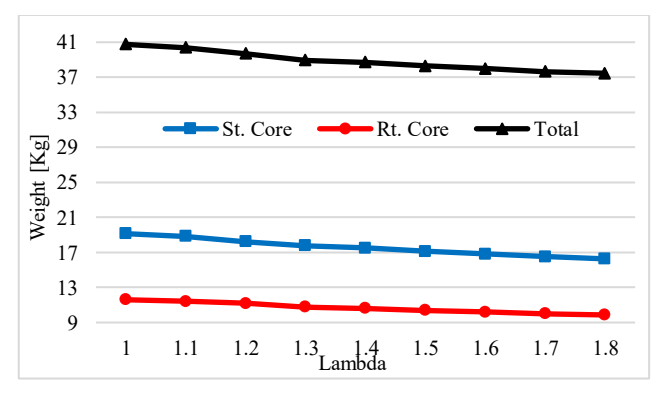


Fig. 9 - Lambda-motor core weight changes.

After geometric calculations and analyses in the design phase, magnetic analyses were performed. In this section, magnetic flux densities, magnetic vector potential changes, transient analyses, torque, and current changes are given for each lambda motor model. In addition, analyses of motor models were made from torque graphs.

In Fig. 10, the magnetic flux density changes for the lambda 1.0 and lambda 1.8 motor models are given. The scale is set to the same value to see the difference between the lambdas. Upon examination of the figure, it is evident that saturation occurs in the stator and rotor teeth and yoke sections due to the geometric decrease in the stator's outer and inner diameter values.

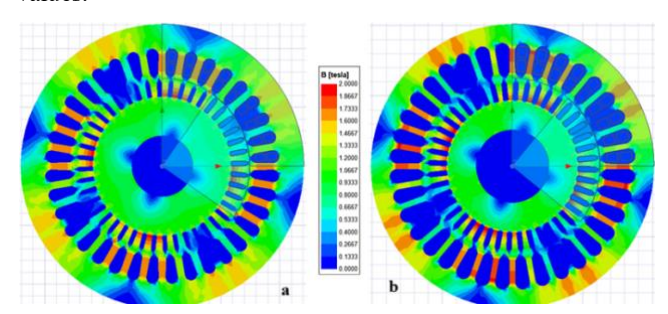


Fig. 10 – Magnetic flux density a) Lambda 1.0 motor model b) Lambda 1.8 motor model.

In Figure 11, the magnetic vector potential changes for the lambda 1.0 and lambda 1.8 motor models are given.

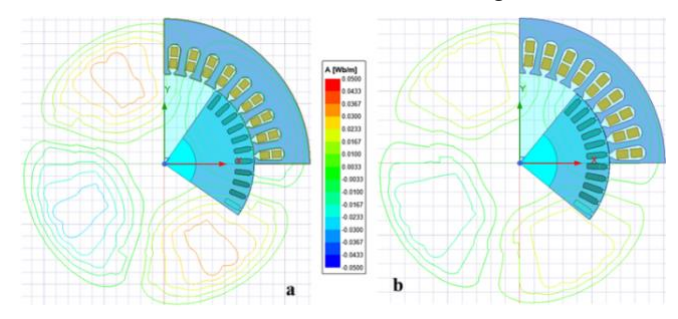


Fig. 11 – Magnetic vector potential changes a) Lambda 1.0 motor model b) Lambda 1.8 motor model

In Fig. 12, torque changes are given for all motor models. As can be seen from the figure, it is seen that oscillations decrease

with the increase of the Lambda value. It is seen that all motor models become more stable at 70 ms.

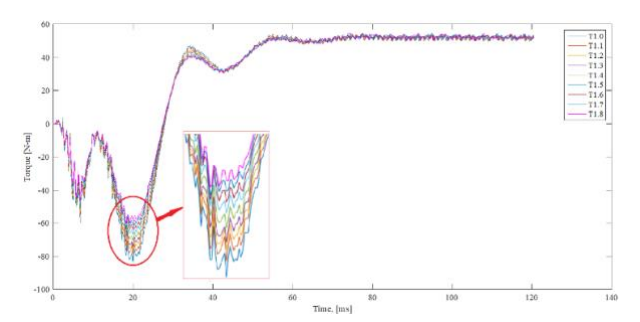


Fig. 12 - Torque changes of motor models at transient moments.

The changes in stator currents of phases A, B, and C for lambda 1.0 and lambda 1.8 are given in Fig. 13.

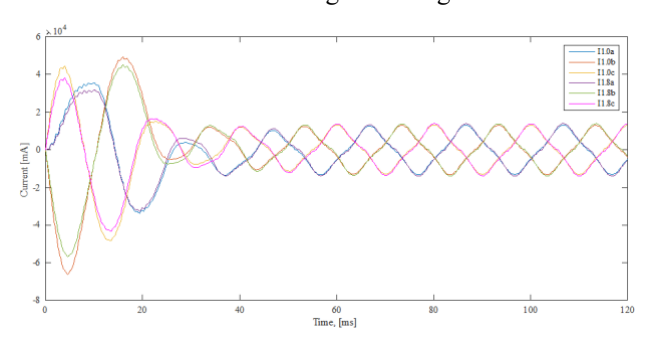


Fig. 13 - Variation of stator currents for Lambda 1.0 and Lambda 1.8.

It is observed that the current value decreases due to the increase in resistance and reactance values with the increase in the lambda value.

The values obtained from the detailed analysis of the torque values obtained from the motor models are given in Table 6. For each motor model, parameters such as minimum, maximum, average values of the torque, torque ripple value, total value and standard deviation were obtained.

Table 6
Various values of torque for each motor model

Lamda	Min.	Max.	Avg.	Ripple	Sum	StdDev
1.0	-84.364	54.269	28.105	136.932	16973.716	38.500
1.1	-79.913	54.035	28.289	132.910	17084.619	37.615
1.2	-76.881	54.051	28.347	130.830	17119.101	37.102
1.3	-74.989	54.106	28.720	127.351	17344.167	36.591
1.4	-71.187	54.108	28.887	123.848	17445.728	35.793
1.5	-67.264	54.065	29.242	119.660	17659.438	35.008
1.6	-64.289	54.139	29.394	117.114	17751.376	34.442
1.7	-62.537	54.287	29.831	113.931	18014.653	34.004
1.8	-60.326	54.492	30.082	111.628	18165.929	33.597

When Table 6 is examined, it is determined that the average torque value increases and the ripple value decreases with the increase in the lambda value. Accordingly, it is seen that the standard deviation decreases. The decrease in ripple is important for the motor to operate more smoothly and stably.

4. PARAMETER ANALYSIS USING TAGUCHI METHOD

The Taguchi method is a widely used method in engineering design. The method's first application in electrical machine design was on the BLDC motor. In recent years, interest in the Taguchi method has rapidly increased, and it has been applied to many electrical machines, including PM synchronous motors, induction motors, reluctance synchronous motors

(RSMs), switched reluctance motors, axial flux PMSMs, and piezoelectric motors. As with all other optimization methods, the number of parameters directly affects the total number of simulations and the complexity of analysing and implementing the final design. In the Taguchi method, existing orthogonal arrays must be considered when selecting the number of parameters for optimization [48].

L16 was used as the orthogonal array in the study. The parameters Dis and L were selected as factors. The Taguchi method is used to determine which values of the inner diameter and package length have the greatest impact on motor design. This is because both the inner diameter and package length directly affect the lambda value. Figure 14 shows the effect of the inner diameter and package length parameters used in motor design on cycle time.

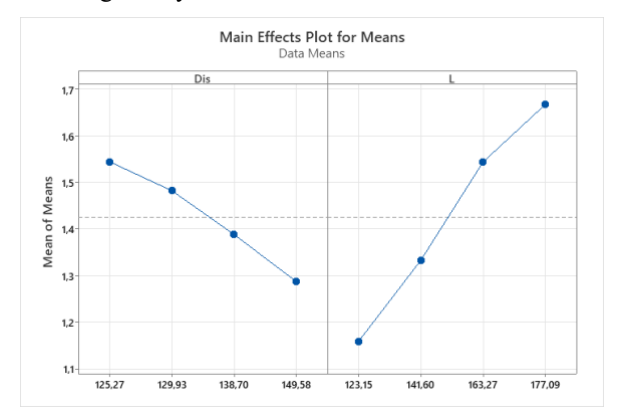


Fig. 14 – Taguchi method mean effect values.

When examining the figure, the inner diameter values of 125.27 mm and 129.93 mm are above the average. For the package length, the values of 163.27 mm and 177.09 mm are above the average. It also means that these values are more effective. This suggests that the induction motor's inner diameter should be smaller, and its package length should be longer. In other words, the lambda value should be higher.

Another analysis in the Taguchi method is the ANOVA analysis and is given in Table 7.

Table 7.
ANOVA table for cycle time

			,			
Source	DF	Adj SS	Adj MS	F-Value	P-Value	
Dis	3	0,150940	0,050313	124,58	0,000	
L	3	0,607299	0,202433	501,24	0,000	
Error	9	0,003635	0,000404			
Total	15	0.761874				

The ANOVA analysis revealed that the inner diameter and package length were statistically significant in terms of cycle time (p<0.05). Furthermore, when the model's accuracy was examined, a very high success rate of 99.52% was achieved, demonstrating that the model worked properly.

5. CONCLUSION

In this study, it was investigated how the lambda parameter, which is not taken into consideration in the design of a three-phase squirrel cage induction motor, affects the motor design and performance. The results obtained showed that the outer and inner diameters of the motor, as well as the package length of the motor, are significantly affected by the lambda parameter. It was determined that the single-phase equivalent circuit parameters of the motor increased with the increase in the lambda value. While the stator and rotor copper losses of the motor increased, a decrease in iron

losses occurred. The nominal torque value almost did not change, and it was concluded that the lambda had no effect on the torque. According to the magnetic analysis results, it was determined that as the lambda value increased, the magnetic flux values increased, and saturations occurred in places. In addition, with the increase in the lambda value, a decrease in the torque oscillations occurred and the average torque value increased. It was observed that the current values were obtained close to each other.

The Taguchi method was used to analyse the inner diameter and package length, which have a direct effect on the lambda parameter. It was concluded that selecting a smaller inner diameter and a larger package length would be more effective for motor design.

If a general evaluation is made, it is seen that the lambda parameter has a great effect on the motor design. Because in the smallest value of lambda, the motor package size is small and the diameter is large, while in the largest value of lambda, the motor package size is large, the diameter is small, and the geometry of the motor is completely changed.

CREDIT AUTHORSHIP CONTRIBUTION STATEMENT

Both authors carried out a literature review, creation and running of models, analytical calculations, performance and magnetic analyses, evaluation and interpretation of studies, compilation and writing of the article, etc. They worked together equally.

Received 8 March 2025

REFERENCES

- M. Abdelwanis and R. El-Sehiemy, Efficient parameter estimation procedure using sunflower optimization algorithm for six-phase induction motor, Rev. Roum. Sci. Techn. – Electrotechn. et Energ., 67, 3, pp. 259–264 (2022).
- H. Benderradji, S. Benaicha, and Y. Laamari, Combined first and second-order sliding mode control of induction motor, Rev. Roum. Sci. Techn. – Électrotechn. Et Energ., 69, 4, pp. 389–394 (2024).
- J. Thankaswamy, M. Paramasivan, M. Rathinam, and U.M. Sundaram, Chaotic randomized space vector pulse width modulation intended for induction motor drives in industrial applications, Rev. Roum. Sci. Techn. – Électrotechn. Et Energ., 69, 4, pp. 401–406 (2024).
- R. Basak and A.K. Paul, Cost-effective design of three-phase induction motor: an optimization approach, Rev. Roum. Sci. Techn. – Électrotechn. et Energ., 67, 4, pp. 461–466 (2022).
- K.S. Deshmukh, K. Bansal, and A. Killedar, *Design and development* of three-phase induction motor using written pole technology, IOSR Journal of Electrical and Electronics Engineering, 11, 5, pp. 49–56 (2016).
- M. Humza and B. Kim, Design of an induction motor by predetermination of equivalent circuit parameters, International Journal of Applied Electromagnetics and Mechanics, 52, pp. 801– 808 (2016).
- R.L. Riese, New aspects of polyphase induction motor design, University of Washington, Doctor of Philosophy (1955).
- P.A. Sakpal and V. Mohale, Design and analysis of a premium efficiency (IE3) induction motor, IJRET: International Journal of Research in Engineering and Technology, 05, 02, pp. 198–203 (2016).
- Y.B. Mandake, Three-phase induction motor -model design and performance analysis in ANSYS RMxprt, International Journal of Scientific Research and Engineering Development, 1, 2, pp. 158– 164 (2018).
- B.M. Dinh, Efficiency improvement of squirrel cage induction motor by rotor slot designs, In Proceedings of the International Conference on Industrial Engineering and Operations Management, Manila, Philippines, pp. 615–623 (2023).
- M.J. Akhtar and R.K. Behera, Optimal design of stator and rotor slot of induction motor for electric vehicle applications, IET Electrical Systems in Transportation, 9, 1, pp. 35–43 (2019).
- 12. M.N. Benallal, M.A. Vaganov, D.S. Pantouhov, E. Ailam, and K. Hamouda, *Optimal value of air gap induction in an induction*

- *motor*, In XIX International Conference on Electrical Machines, Rome, Italy, pp. 1–4 (2010).
- I. Boldea, Induction Machines Handbook: Transients, Control Principles, Design and Testing, Motor Specifications and Design Principles, CRC Press (2020).
- M. Aishwarya and R.M. Brisilla, Design of energy-efficient Induction motor using ANSYS software, Results in Engineering, 16, pp. 1–10 (2022).
- I.K. Onwuka, P.I. Obi, O. Oputa, and C.S. Ezeonye, Performance analysis of induction motor with variable air-gaps using finite element method, NIPES Journal of Science and Technology Research, 5, 1, pp. 112–124 (2023).
- C. Saravanan, A.M. Azarudeen, and S. Selvakumar, Performance of three-phase induction motor using modified stator winding, Global Journal of Research in Engineering Electrical and Electronics Engineering, 12, 5, pp. 1–6 (2012).
- Z. Anthony, S. Bandri, E. Erhaneli, Y. Warmi, Z. Zulkarnaini, and A.Y.D. Rachman, A winding design for improving 3-phase induction motor performance, International Journal of Electrical and Computer Engineering (IJECE), 14, 3, pp. 2413–2421 (2024).
- E. El-Kharashi and M. El-Dessouki, Coupling induction motors to improve the energy conversion process during balanced and unbalanced operation, Energy, 65, pp. 511–516 (2014).
- I.M.W. Kastawan, P. Raharjo, R.D. Kusumah, and M.Z. Kurnia, Effect of voltage supply unbalance on vibration of three-phase induction motor, Journal of Physics: Conference Series, 2828, pp. 1–8 (2024).
- M. Ozsoy, O. Kaplan, and M. Akar, FEM-based analysis of rotor cage material and slot geometry on double air gap axial flux induction motors, Ain Shams Engineering Journal, 15, pp. 1–13 (2024).
- D.T. McGuiness, M.O. Gülbahce, and D.A. Kocabas, Novel rotor design for high-speed solid rotor induction machines, In 9th International Conference on Electrical and Electronics Engineering (ELECO), Bursa, Türkiye, pp. 579–583 (2015).
- M.Ş. Kurt and A. Fenercioğlu, Effect of the variable resistance rotor slot design on the performance of the single-phase asynchronous motor (SPAM), Sigma Journal of Engineering and Natural Sciences, 38, 1, pp. 213–226 (2020).
- T.M. Masuku, R.J. Wang, M.C. Botha, and S. Gerber, *Design strategy of traction induction motors*, In Proc. the 27th Southern African Universities Power Engineering Conference, Bloemfontein, South Africa, pp. 316–321 (2019).
- K. Li, G. Cheng, X. Sun, Z. Yang, and Y. Fan, Performance optimization design and analysis of bearingless induction motor with different magnetic slot wedges, Results in Physics, 12, pp. 349–356 (2019).
- A.I.S. Juhaniya, A.A. Ibrahim, M.A.A.M. Zainuri, M.A. Zulkifley, and M.A. Remli, Optimal stator and rotor slots design of induction motors for electric vehicles using opposition-based jellyfish search optimization, Machines, 10, pp. 1–18 (2022).
- M.Ş. Kurt and A. Fenercioğlu, Rotor slot distance effects on output parameters in single-phase induction motors, Hittite Journal of Science and Engineering, 5, 1, pp. 31–35 (2018).
- A.I.S. Juhaniya, A.A. Ibrahim, M.A.A.M. Zainuri, and M.A. Zulkifley, *An analytical model of induction motors for rotor slot parametric design performance evaluation*, International Journal of Advanced Computer Science and Applications, 13, 12, pp. 883–889 (2022).
- M.R. Nakhaei and R. Roshanfekr, Optimal design of 3-phase squirrel cage induction motors using genetic algorithm based on the motor efficiency and economic evaluation of the optimal model, Balkan Journal of Electrical & Computer Engineering, 9, 1, pp. 59–68 (2021).
- H. Manani, Design optimization of 3-phase induction motor, GIT-Journal of Engineering and Technology, 14, pp. 84–90 (2022).
- M. Dems, S. Lachecinski, and S. Wiak, *Influence of the constraints on the optimal problem solution using particle swarm algorithm*, Przeglad Elektrotechniczny, 86, 8, pp. 127–130 (2010).
- P.K. Ghosh and P.K. Sadhu, Discrete design optimization of a 3-phase squirrel cage type induction motor, Journal of University of Shanghai for Science and Technology, 24, 2, pp. 169–181 (2022).
- G. Joksimovi, E. Levi, A. Kajevi, M. Mezzarobba, and A. Tessarolo, Optimal selection of rotor bar number for minimizing torque and current pulsations due to rotor slot harmonics in three-phase cage induction motors, IEEE Access, 8, pp. 1–14 (2020).
- A. Eke, G. Fischer, A. David, O. Ekpenyong, and E.J. Akpama, The
 effect of rotor and stator slot numbers on the performance of threephase induction motors used for transport application, IOSR
 Journal of Electrical and Electronics Engineering, 19, 4, pp. 01–09
 (2024).
- 34. M. Valtonen, A. Parviainen, and J. Pyrhonen, The effects of the number

- of rotor slots on the performance characteristics of axial-flux aluminium-cage solid-rotor core induction motor, In IEEE International Electric Machines & Drives Conference, Antalya, Türkiye, pp. 668–672 (2007).
- H. Nory, A. Yildız, S. Aksun, and C. Aksoy, Influence of stator and rotor slots combination on induction motor performance, In IEEE Third International Conference on Power Electronics, Intelligent Control and Energy Systems, Delhi, India, pp. 177–181 (2024).
- F. Mahmouditabar and N.J. Baker, Design optimization of induction motors with different stator slot rotor bar combinations considering drive cycle, Energies, 17, pp. 1–25 (2024).
- M.V. Terzic, D.S. Mihic, and S.N. Vukosavic, Stator design and air gap optimization of high-speed drag-cup induction motor using FEM, Advances in Electrical and Computer Engineering, 13, 3, pp. 93–100 (2013).
- 38. M. Muteba, Optimization of air gap length and capacitive auxiliary winding in three-phase induction motors based on a genetic algorithm, Energies, 14, pp. 1–18 (2021).
- M. Muteba and D.V. Nicolae, Influence of air-gap length on the performance of a three-phase induction motor with a capacitive auxiliary stator winding, In 44th Annual Conference of the IEEE Industrial Electronics Society, Washington, DC, USA, pp. 547– 552 (2018).

- User's Guide Maxwell 2D, Electronic design automation software, pp. 1–628 (2010).
- I. Boldea and S.A. Nasar, The Induction Machine Handbook, CRC Press LLC, Washington, D.C. (2001).
- J. Legranger, G. Friedrich, and R. Trigui, Integration of an induction machine synthesis in a multiphysic simulation tool for automotive applications, In Third International Conference on Ethnomathematics, Auckland, France, pp. 1–6 (2006).
- 43. I. Boldea and S.A. Nasar, *The Induction Machines Design Handbook*, Second Edition, CRC Press, USA (2010).
- O.I. Olubamiwa, Design of a Rotor-tied doubly fed induction generator,
 University of Stellenbosch, Department of Electrical and Electronic Engineering, South Africa (2017).
- S.P. Barave and B.H. Chowdhury, Optimal design of induction generators for space applications, IEEE Transactions on Aerospace and Electronic Systems, 45, 3, pp. 1126–1137 (2009).
- O. Gürdal, Design of electrical machines, Bursa Orhangazi Üniversitesi Yayınları, Bursa, Türkiye (2015).
- 47. A.K. Sawhney, A Course in Electrical Machine Design, India (2016).
- 48. A. Sorgdrager, R. JieWang, and A. Grobler, *Taguchi Method in Electrical Machine Design*, South African Institute of Electrical Engineers, **108**, 4, pp. 150–164 (2017).